Ab Initio Evaluation of Plutonium Dioxide $S(\alpha,\beta)$ and Thermal Neutron Cross Sections

J. P. W. Crozier, A. I. Hawari

Department of Nuclear Engineering, North Carolina State University, Raleigh, NC 27695, USA
jpcrozie@ncsu.edu , ayman.hawari@ncsu.edu

INTRODUCTION

Plutonium Dioxide (PuO_2) is an advanced fuel-cycle nuclear fuel material for thermal and fast reactors, with a melting point at 3261.8 K and thermal conductivity above 3 $Wm^{-1}K^{-1}$ for temperatures below 1500 K [1]. Plutonium from spent UO_2 is reprocessed to form chemically stable mixed-oxide (MOX) fuel. In contrast to metallic fuels, the low PuO_2 conductivity results in high thermal gradients between fuel center and surface, resulting in structural annealing and efficient fission product migration over burnup [2].

Crystal binding affects the doppler broadening of epithermal resonances for nuclear fuels [3] and scattering behavior of thermal neutrons [4]. Currently, there is no ENDF/B Thermal Scattering Law, i.e., $S(\alpha,\beta)$, evaluation for PuO_2, only free atom cross sections for Plutonium and Oxygen, respectively, which neglect lattice contributions to total cross section. Herein, *ab initio* lattice dynamics (AILD) techniques are employed to calculate the phonon density of states (DOS) using spin-orbit-coupling density functional theory (DFT) to predict the PuO_2 paramagnetic ground-state structure.

These results highlight the evaluation of $S(\alpha,\beta)$ for Plutonium and Oxygen, respectively in PuO_2 and consequential generation of thermal neutron scattering cross sections for high fidelity criticality safety analysis and reactor calculations.

THERMAL SCATTERING LAW THEORY

The thermal neutron de-Broglie wavelength is on the order of magnitude of inter-atomic spacing and its energy is on the order of magnitude of lattice vibrations. The thermal scattering interactions in a crystalline material is therefore a function of its structure and vibrational state availability: inelastic scattering energy can be transferred to absorption and emission of elementary excitations (phonons), and elastic scattering is identified by Bragg edges.

The following form of the double-differential inelastic scattering cross section of thermal neutrons describes the reaction rate of neutron with energy E scattering through a solid angle Ω to energy E' as [5]:

$$\frac{\partial^2\sigma}{\partial\Omega\partial E'} = \frac{1}{4\pi k_B T}\sqrt{\frac{E'}{E}}\left[\sigma_{coh}S(\alpha,\beta) + \sigma_{inc}S_s(\alpha,\beta)\right] \quad (1)$$

Therefore, in the first Born approximation, the scattering probability is defined by coherent and incoherent cross sections, σ_{coh} and σ_{inc}. The thermal scattering law, $S(\alpha,\beta)$, is an inherent description of the scattering system as a function of dimensionless momentum and energy exchange parameters, α and β:

$$S(\alpha,\beta) = S_s(\alpha,\beta) + S_d(\alpha,\beta) \quad (2)$$

In this form [4], the TSL can be decomposed into *self* and *distinct* components, where S_s describes non-interference lattice effects. In the incoherent approximation, the *distinct* interference lattice effects between atoms in the scattering system are neglected, implying that nuclei behave as independent oscillators for inelastic scattering [6]:

$$\frac{\partial^2\sigma}{\partial\Omega\partial E'} = \frac{1}{2\pi k_B T}\sqrt{\frac{E'}{E}}\left[\sigma_{coh} + \sigma_{inc}\right] S_s(\alpha,\beta) \quad (3)$$

In the case of PuO_2, the coherent scattering lengths for ^{238}Pu, ^{239}Pu, and ^{240}Pu are 14.1, 7.7 and 3.5 fm, while the incoherent scattering lengths are 0, ±1.3, and 0 fm [7]. The coherent scattering lengths for ^{16}O, ^{17}O and ^{18}O are 5.803, 5.78 and 5.84, while the incoherent scattering lengths are 0, 0.18 and 0 [7]. The incoherent inelastic cross section is therefore calculated with a phonon expansion in the harmonic approximation and the coherent elastic double differential cross section can be calculated as a function of the atomic structure factor in the cubic approximation. Bose-Einstein statistics determine availability of lattice vibrations.

COMPUTATIONAL METHODS

PuO_2 has a fluorite-type crystal structure, equivalent to that of CaF_2, with $Fm\bar{3}m$ symmetry (space group 225), liken to that of other actinide dioxides [8]. PuO_2 is paramagnetic (PM) for experimentally accessible temperatures [9], which differs from the low-temperature transitions to anti-ferromagnetic and multi-pole ordering of Uranium Dioxide [10]. Electronically, PuO_2 is characterized as a Mott-Hubbard insulator on account of the strong correlation between 5*f* orbital electrons [11].

Electronic structure minimization for the longitudinal AFM-1K ground state is conducted using VASP [12,13]. These calculations assume the spin-orbit-coupling (SOC) formalism with PAW pseudopotentials and the GGA-PBEsol

exchange-correlations [14]. A plane-wave cut-off of 500 eV, 9x9x9 Monkhorst-Pack k-mesh and Gaussian smearing width of 0.02 eV ensure that the ground state energy and volume converge to below 5 meV/atom and 0.1%, respectively [15]. Additionally, a moderate effective Hubbard value (U-J) of 4 eV controls the degree of Plutonium *5f* orbital electron itineracy [16,10].

2x2x2 cubic supercell calculations (containing 32 Plutonium and 64 Oxygen atoms) displace non-equivalent Plutonium and Oxygen sites by 0.03 Å in $\pm\vec{x}$. The isotropic PM phase is approximated by weighting the Hellmann-Feynman forces (HFF) for varying transverse AFM-1K magnetic configurations [17]. Phonon dispersion relations and partial DOS are calculated in PHONON [18] from HFFs and processed in *FLASSH* (Full Law Scattering System Hub) [19] to evaluate $S(\alpha,\beta)$, incoherent inelastic and coherent elastic cross sections for Plutonium and Oxygen in PuO_2.

The predicted DOS can be compared against experimental data by neutron-weighting the AILD partial DOS. The electronic density of states can be evaluated with respect to the experimental band gap of 1.8 eV [20] and x-ray photoemission spectroscopy (XPS) data [21]. These calculations assume natural isotopic abundances for Oxygen, and Plutonium isotopics characteristic of MOX fuel fabricated from pressurized water reactor (PWR) spent fuel at 43 MW day/kg [22]. Isotope-specific free-atom cross sections and masses correspond with current ENDF/B-VIII data [23]. The total thermal scattering cross section of PuO_2 calculated in *FLASSH* can be combined with absorption cross sections for comparison against experimental transmission data [24].

RESULTS AND DISCUSSION

Plutonium Dioxide's ground-state, paramagnetic crystal structure is approximated by averaging the dynamical contributions from orthogonal, transverse 1K anti-ferromagnetic (AFM-1K) configurations. Using *VESTA* [25], Figure 1 shows the transverse AFM-1K PuO_2 unit-cell structure with the Plutonium dipoles oriented along $\vec{c}$. The black and red sites represent Plutonium and Oxygen, respectively, and the green and purple arrows denote the direction of Plutonium's magnetic moment:

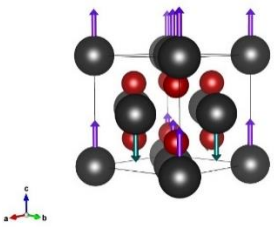

Fig. 1 PuO_2 Crystal Structure

The predicted structure demonstrates excellent agreement with the experimental lattice parameter in Table I. The slight over-estimation agrees with result from similar GGA+U frameworks [9] and is important in predicting Oxygen's high-frequency phonon modes which are sensitive to inter-atomic spacing.

TABLE I. PuO_2 DFT-Predicted Structural Properties

Lattice Parameter	AILD	Experiment [25]	Deviation (%)
a (Å)	5.4011	5.3975	0.07

Figure 2 demonstrates that the AILD electronic DOS predicts a band gap of 1.729 eV, which compares well with the experimentally determined value of 1.8 eV [21]. This agreement suggests that the present model accurately characterizes Plutonium's correlated 5*f* orbital interactions above the fermi energy, E_F, for the PuO_2 insulating ground-state:

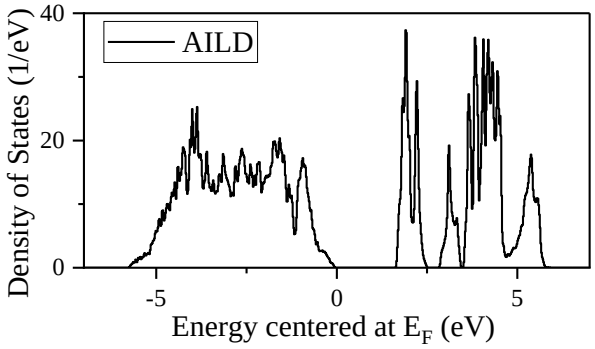

Fig. 2. PuO_2 predicted electronic DOS

Dynamically, Oxygen frequencies mainly dominate the high energy longitudinal optic (LO) and transverse optic (TO) modes, while the longitudinal and transverse acoustic (LA,TA) modes are dominated by Plutonium. This is exemplified by phonon dispersion relations in Figure 3:

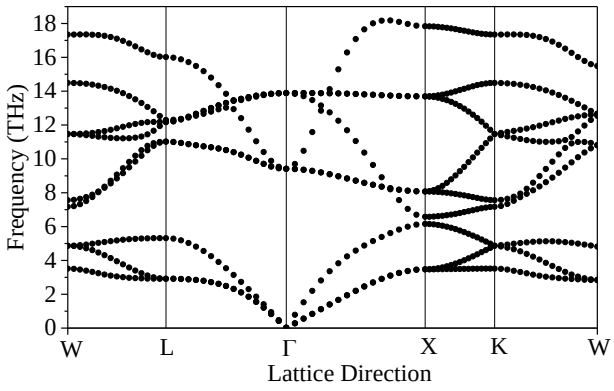

Fig. 3. PuO_2 phonon dispersion relations

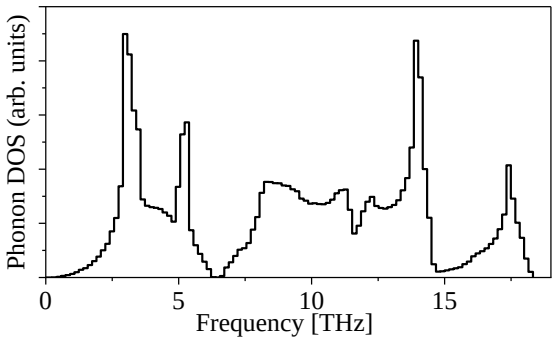

Fig. 4. PuO_2 total phonon DOS

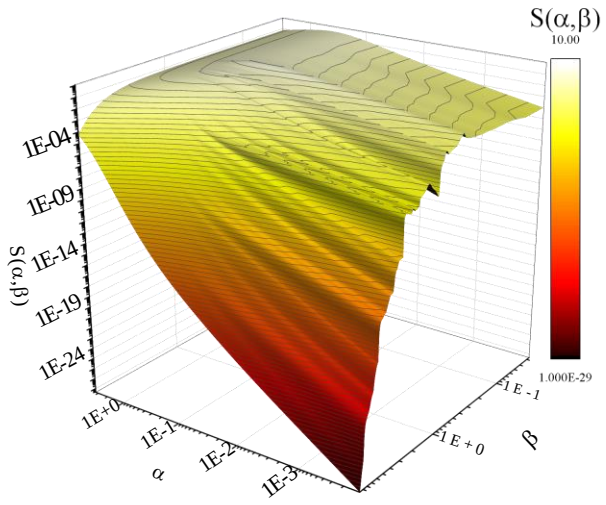

Fig. 5. Plutonium in PuO_2 $S(\alpha,\beta)$ at 296 K

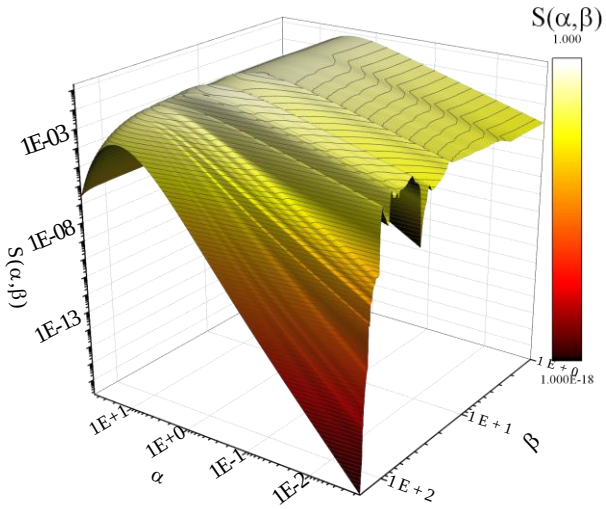

Fig. 6. Oxygen in PuO_2 $S(\alpha,\beta)$ at 296 K

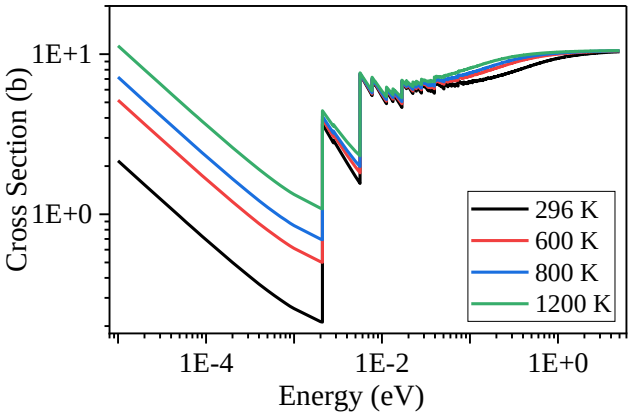

Fig. 7. Total thermal scattering cross sections for Plutonium in PuO_2 at varying temperatures

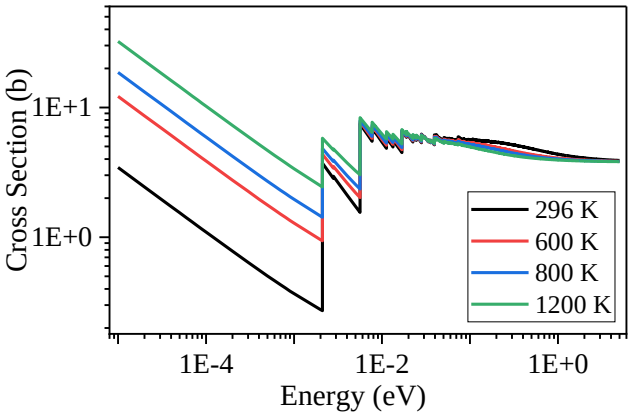

Fig. 8. Total thermal scattering cross sections for Oxygen in PuO_2 at varying temperatures

The generalized phonon spectrum demonstrates good agreement with time of flight (TOF) measurements and the individual contributions from partial phonon DOS are used to calculate $S(\alpha,\beta)$ in *FLASSH*. The total phonon DOS is presented in Figure 4.

The Plutonium and Oxygen in PuO_2 $S(\alpha,\beta)$ distributions along β are characteristic of their respective phonon DOS features, as per Figures 5 and 6. The Oxygen in PuO_2 $S(\alpha,\beta)$ does not display quantum oscillatory behavior like those exhibited in hydrides and actinide nitrides [17].

In Figures 7 and 8, the total thermal scattering cross sections are dominated by inelastic scattering below .005 eV, after which elastic scattering peaks occur at Bragg edges. The total scattering cross sections for both Plutonium and Oxygen in PuO_2 asymptotically approach their respective free-atom cross sections. By including neutron absorption interactions, the total calculated cross section can be compared with neutron transmission data in the thermal energy range.

CONCLUSIONS

The present work accurately predicts PuO_2's ground state magnetic structure and semi-itinerant 5*f* orbital interactions with a spin-orbit coupling, GGA+U methodology: predicted lattice parameter, electronic DOS and phonon DOS agree well with experimental data.

Plutonium and Oxygen's respective partial phonon density of states allow for the novel evaluation of their thermal scattering laws, and first-principles generation of coherent elastic and incoherent inelastic cross sections, thus accounting for lattice binding contributions to low energy neuron scattering interactions.

ACKNOWLEDGMENT

This work was partially funded by the US National Nuclear Security Administration's (NNSA) Nuclear Criticality Safety Program (NCSP).

REFERENCES

1. C. COZZO et al., "Thermal diffusivity and conductivity of thorium-plutonium oxides," *Journal of Nuclear Materials,* 416 (2011)
2. J. H. KITTEL et al., "History of fast reactor fuel development," *Journal of Nuclear Materials*, 204 (1993)
3. J. P. W. CROZIER, N. C. FLEMING and A. I. HAWARI, "Thermal scattering law for structure-dependent doppler broadening in *FLASSH*," *PHYSOR-Making Virtual a Reality*, Pittsburgh, PA (2022)
4. J. P. W. CROZIER and A. I. HAWARI, "Ab initio evaluation of uranium carbide $S(\alpha,\beta)$ and thermal neutron cross sections," *15th International Conference on Nuclear Data for Science and Technology*, Sacramento, CA (2022)
5. G. SQUIRES, *Introduction to the Theory of Thermal Neutron Scattering*, Cambridge University Press, UK (1978)
6. A.I. HAWARI, "Modern techniques for inelastic thermal neutron scattering analysis," *Nuclear Data Sheets* 118 (2014)
7. V. F. SEARS, "Neutron scattering lengths and cross sections," *Neutron News*, 3 (1992)
8. J. L. WORMALD, N. C. FLEMING, A. I. HAWARI and M. L. ZERKLE, "Generation of the thermal scattering law of uranium dioxide with ab initio lattice dynamics to capture crystal binding effects on neutron interactions," *Nuclear Science and Engineering*, 195 (2021)
9. G. RAPHAEL and R. LALLEMENT, "Susceptibilitie magnetique de PuO_2," *Solid State Communications,* 6 (1968)
10. H. NAKAMURA et al., "Effects of spin-orbit coupling and strong correlation on the paramagnetic insulating state in plutonium dioxides," *Physical Review B,* 82 (2010)
11. H. NAKAMURA et al., "First-principles calculation of phonon and Schottky heat capacities of plutonium dioxide," *Journal of the Physical Society of Japan*, 84 (2015)
12. G. KRESSE and D. JOUBERT, "From ultrasoft pseudopotentials to the projector augmented-wave method," *Physical Review B,* **59** 1785 (1999)
13. G. KRESSE and J. HAFNER, "Ab initio molecular dynamics for liquid metals," *Physical Review B,* **47** 558 (1993)
14. J. PERDEW et al., "Generalized gradient approximation made simple," *Physical Review Letters,* **77** 18 (1996)
15. H. J. MONKHORST and J. D. PACK, "Special points for Brillouin-zone integrations," *Physical Review B,* **13** (1976).
16. S. DUDAREV et al., "Electron-energy-los spectra and structural stability of nickel oxide: an LSDA+U study," *Physical Review B,* **57** (1998)
17. J. L. WORMALD, A. I. HAWARI and M. L. ZERKLE, "Impact of magnetic structure and thermal effects on vibrational excitations and neutron scattering in uranium mononitride," *Annals of Nuclear Energy*, 143 (2020)
18. K. PARLINSKI et al., "First-principles determination of the soft mode in cubic ZrO2," *Physical Review Letters,* **78** 4063 (1997).
19. N. C. FLEMING, C. A. MANRING, B. K. LARAMEE, J. P. W. CROZIER and A. I. HAWARI, "*FLASSH1.0*: Thermal scattering law evaluation and cross section generation," *PHYSOR- Making Virtual a Reality*, Pittsburgh, PA (2022)
20. C. E. MCNEILLY, "The electrical properties of plutonium oxides," *Journal of Nuclear Materials*, 11 (1964)
21. D. COURTEIX et al., "XPS study of plutonium oxides," *Solid State Communications,* 39 (1981)
22. S. FEHER et al., "MOX fuel effects on the isotope inventory in LWRs," *Nuclear Engineering and Design*, 252 (2012)
23. D. A. BROWN et al., "ENDF/B-VIII.0: The 8th major release of the nuclear reaction data library with CIELO-project cross sections, new standards and thermal scattering data," *Nuclear Data Sheets*, 148 (2018)
24. N. J. PATTENDEN, "The slow neutron total cross section of plutonium," *Journal of Nuclear Energy*, 2 (1956)
25. K. MOMMA and F. IZUMI, "*VESTA*: a three-dimensional visualization system for electronic and structural analysis," *Journal of Applied Crystallography*, 41 (2008)